Supporting Information

Bimetallic MOF-Derivatives Enabled Multi-Sited Current Collector for High-Performance Anode-Free Lithium Metal Battery

Rui Luo [a], Xingtong Guo [a], Zi Wang [a], Xiaonuo Jiang [a], Chao Su [a], Tao Wei [a,*]

[a] *School of Energy and Power, Jiangsu University of Science and Technology, Zhenjiang 212100, China.*

1. Experimental section

1.1 Chemicals

Nickel(II) nitrate hexahydrate ($Ni(NO_3)_2·6H_2O$, AR, 99%, Aladdin), Cobalt(II) nitrate hexahydrate ($Co(NO_3)_2·6H_2O$, 99.9%), 1,3,5-Benzenetricarboxylic acid (BTC, 99%, Aladdin), Polyvinylpyrrolidone (PVP, 99%, Aladdin), Carbon Cloth (Hesen Tech Co., Ltd.), N, N-Dimethylformamide (DMF, 99.8%, Aladdin). All solvents and chemicals can be utilized directly without the need for additional purification.

1.2 Preparation of CC@Ni/CoO

The pre-cleaned carbon cloth was immersed in a solution containing $Ni(NO_3)_2·6H_2O$, $Co(NO_3)_2·6H_2O$, BTC, PVP, and DMF in a defined molar ratio (specifically: 582 mg $Ni(NO_3)_2·6H_2O$, 582 mg $Co(NO_3)_2·6H_2O$, 300 mg BTC, 1 g PVP, and 60 mL DMF). The mixture was then transferred into a Teflon-lined autoclave and subjected to hydrothermal treatment at 160°C for 10 h to obtain CC@NiCo-MOFs. The wet

* Corresponding author: T. Wei (wt863@just.edu.cn; wt863@126.com).

CC@NiCo-MOFs was subsequently dried in an oven at 80°C. Thereafter, the as-prepared CC@NiCo-MOFs were first heated at 400 °C for 2 h and then carbonized at 800 °C for an additional 2 h under N_2 atmosphere to obtain CC@Ni/CoO.

1.3 Preparation of Li-CC@Ni/CoO

Then, a lithium foil and CC@Ni/CoO were placed in the furnace, and molten lithium was injected into the CC@Ni/CoO from bottom to top, resulting in the formation of Li-CC@Ni/CoO (Fig. S6).

1.4 Materials characterization

The crystalline phase of the Ni/CoO powder was examined using an X-ray diffractometer (XRD, Bruker D8 Advance). X-ray photoelectron spectroscopy (XPS) data were collected on an AXIS ULTRA DLD spectrometer. Surface microstructures were observed with a field-emission scanning electron microscope (SEM, Hitachi Regulus-8100), and elemental compositions/mappings were determined by energy-dispersive spectroscopy (EDS). The microstructure of the sample was further characterized by transmission electron microscopy (Titan G2 spherical aberration corrected TEM, FEI company, 80-300kV).

1.5 Electrochemical measurement

Electrochemical measurements were conducted in CR2032 coin-type cells. Lithium foil served as the reference/counter electrode; half-cells employed CC@Ni/CoO as the working electrode, whereas symmetric cells used two identical Li-CC@Ni/CoO electrodes. Full cells were assembled with Li-CC@Ni/CoO as the anode and $LiFePO_4$

(LFP) as the cathode. The LFP cathode sheet was prepared by mixing 70 wt % lithium iron phosphate, 20 wt % acetylene black and 10 wt % poly (vinylidene fluoride) into N-methyl-2-pyrrolidone to form a homogeneous slurry that was evenly coated onto clean aluminum foil, dried at 60°C for 3h, and further vacuum-dried at 120°C for 12h. The resulting film was punched into 16mm diameter disks. For anode-free full cells, Kelude LF06XX high-mass-loading cathodes (~12.3 mg cm^{-2}) were used. A Celgard 2500 polypropylene membrane acted as the separator. The electrolyte for full cells was 1.0 M $LiPF_6$ in EC:DMC:EMC (1:1:1 wt%); half-cells and symmetric cells utilized 1.0 M LiTFSI in DME:DOL (1:1 vol%) containing 20% $LiNO_3$.

Long-term galvanostatic cycling was performed on a LAND CT2001A battery test system (Wuhan Jinnuo Electronics, China). Electrochemical impedance spectroscopy (EIS) was recorded at room temperature with a CHI-660E electrochemical workstation (Shanghai Chenhua Instrument) over the frequency range of 10^6 Hz to 10^1 Hz.

2. Experimental data

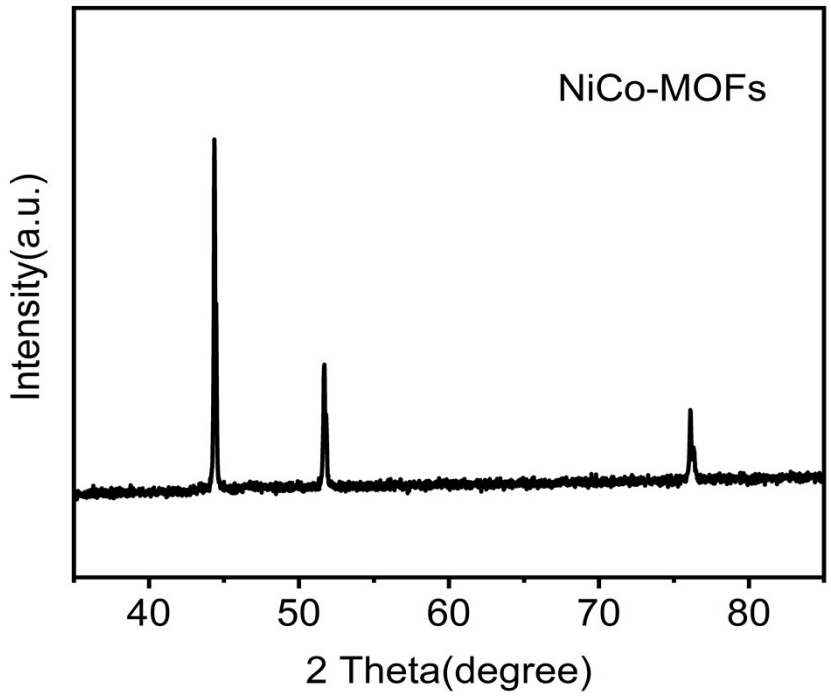

Fig. S1 XRD of NiCo-MOFs

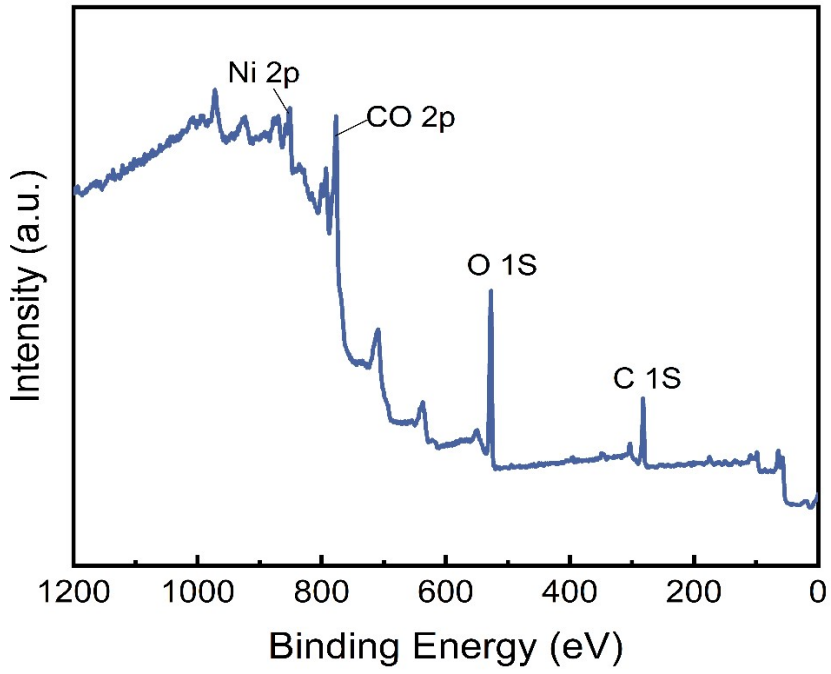

Fig. S2 XPS spectra of NiCo-MOFs derived Ni/CoO

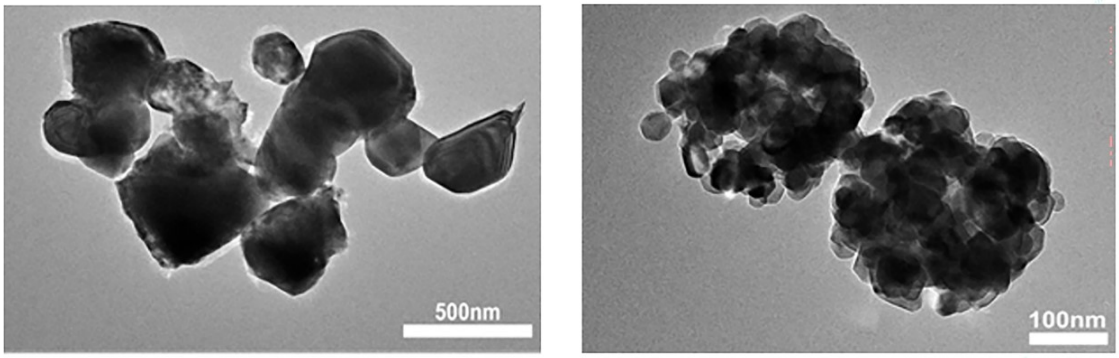

Fig. S3 TEM image of Ni/CoO

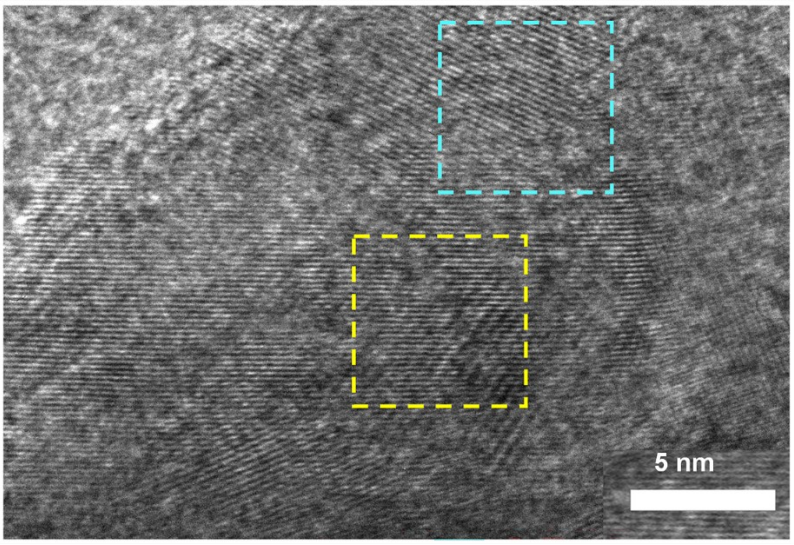

Fig. S4 HRTEM image of Ni/CoO

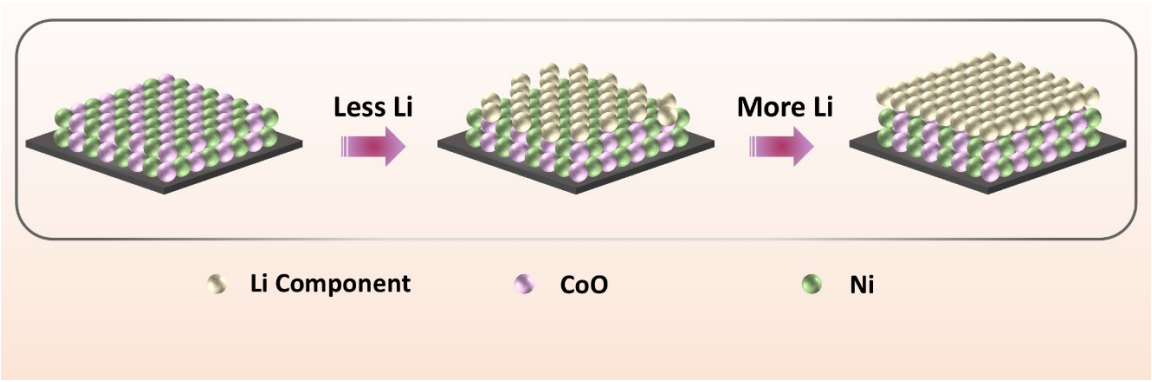

Fig. S5 Mechanism diagram of the intermittent deposition of lithium

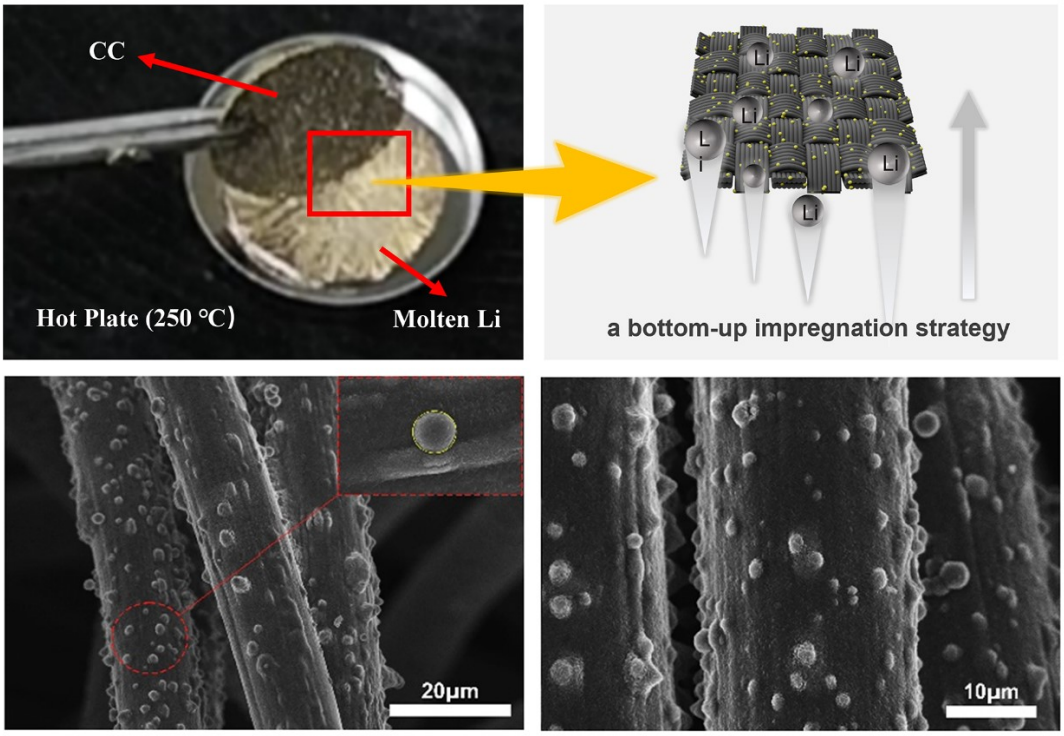

Fig. S6 Preparation of the Li-CC@Ni/CoO electrode

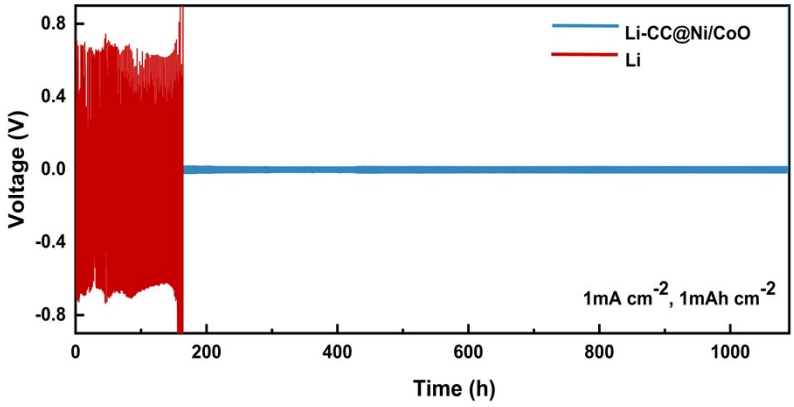

Fig. S7 Cycling performance of symmetric cells (Li-CC@Ni/CoO||Li-CC@Ni/CoO and Li||Li) as a function of current density and areal capacity at 1 mA cm^{-2} ,1 mAh cm^{-2}

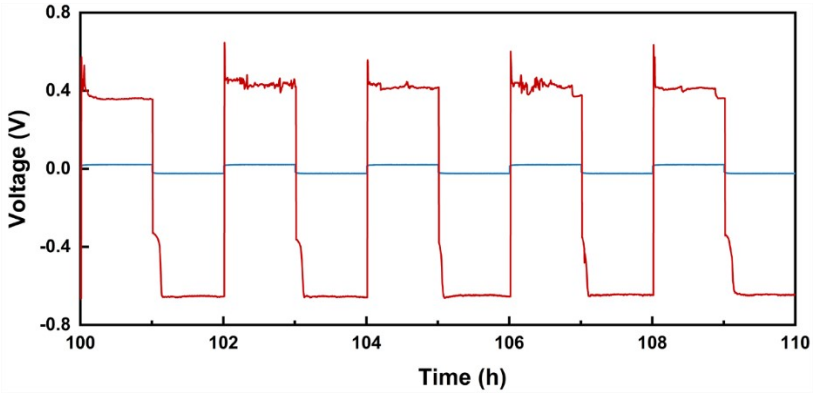

Fig. S8 Li-CC@Ni/CoO||Li-CC@Ni/CoO symmetric cell cycled at 1 mA cm^{-2} and 1 mAh cm^{-2}

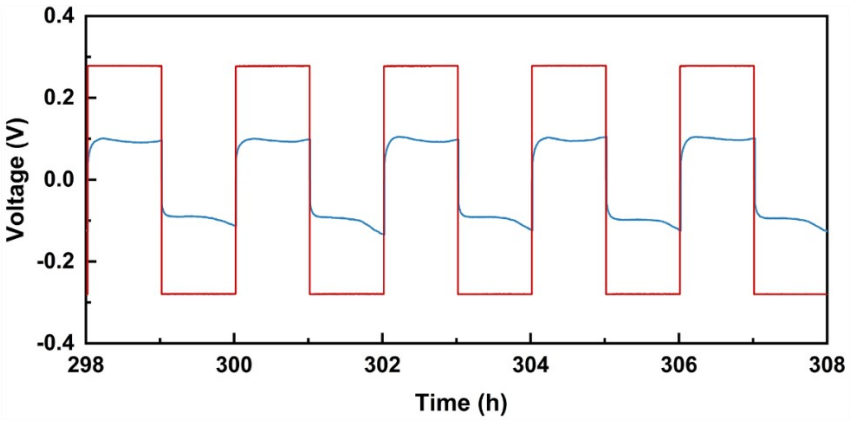

Fig. S9 Li-CC@Ni/CoO||Li-CC@Ni/CoO symmetric cell cycled at 3 mA cm^{-2} and 3 mAh cm^{-2}

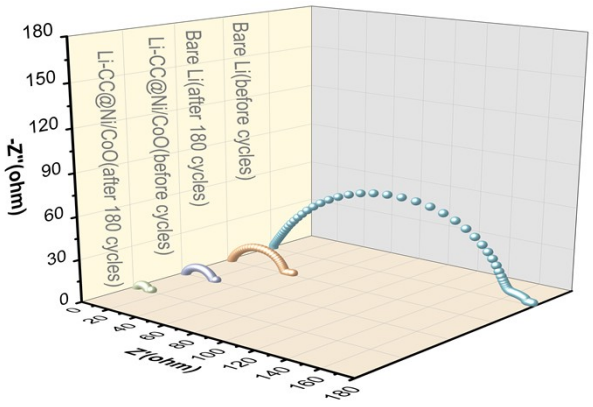

Fig. S10 Initial and post-cycling (after 180 cycles) EIS spectra of the symmetric cells.

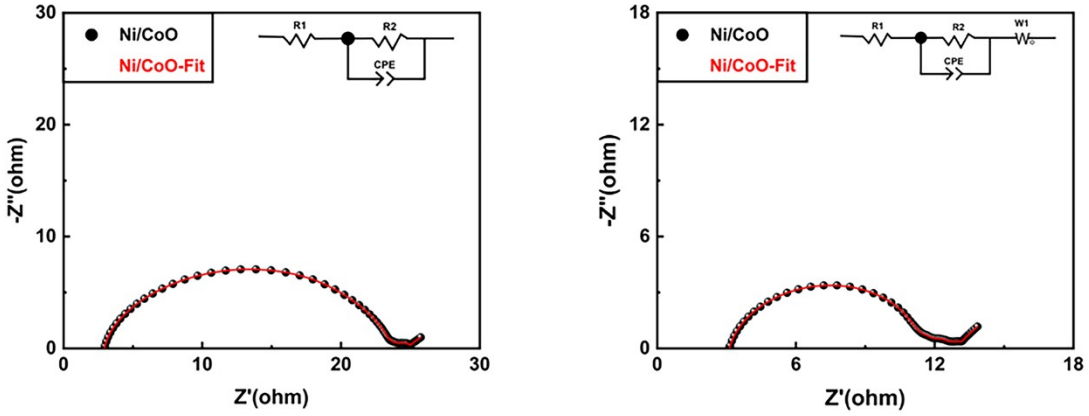

Fig. S11 Nyquist plot and corresponding fitting curve of the Li-CC@Ni/CoO||Li-CC@Ni/CoO cell. (a)before cycles(b)after 180 cycles

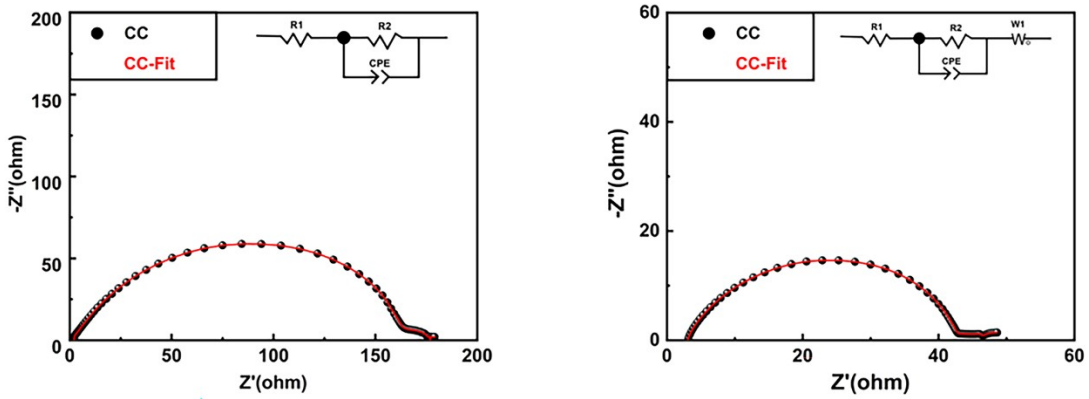

Fig. S12 Nyquist plot and corresponding fitting curve of the Li||Li cell. (a)before cycles(b)after 180 cycles

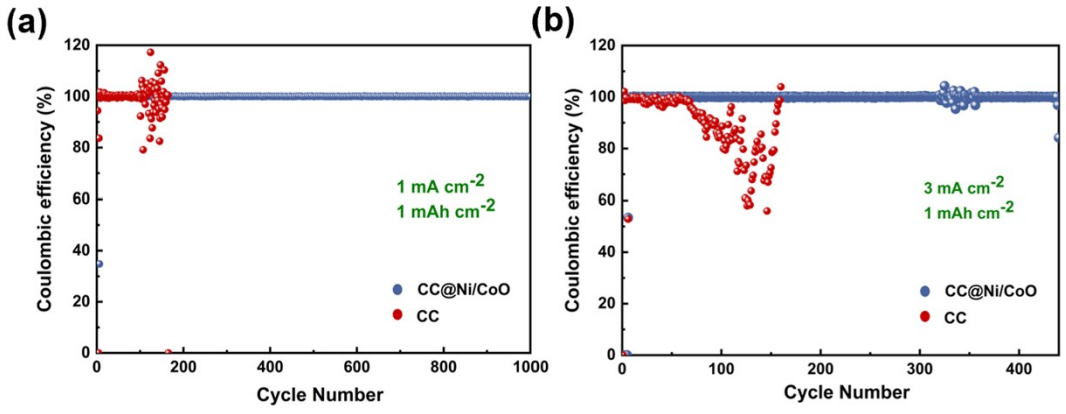

Fig. S13 CE of the CC and CC@Ni/CoO electrodes at current densities of (a) 1 mA cm^{-2}, (b) 3 mA cm^{-2}, under a fixed areal capacity of 1 mAh cm^{-2}

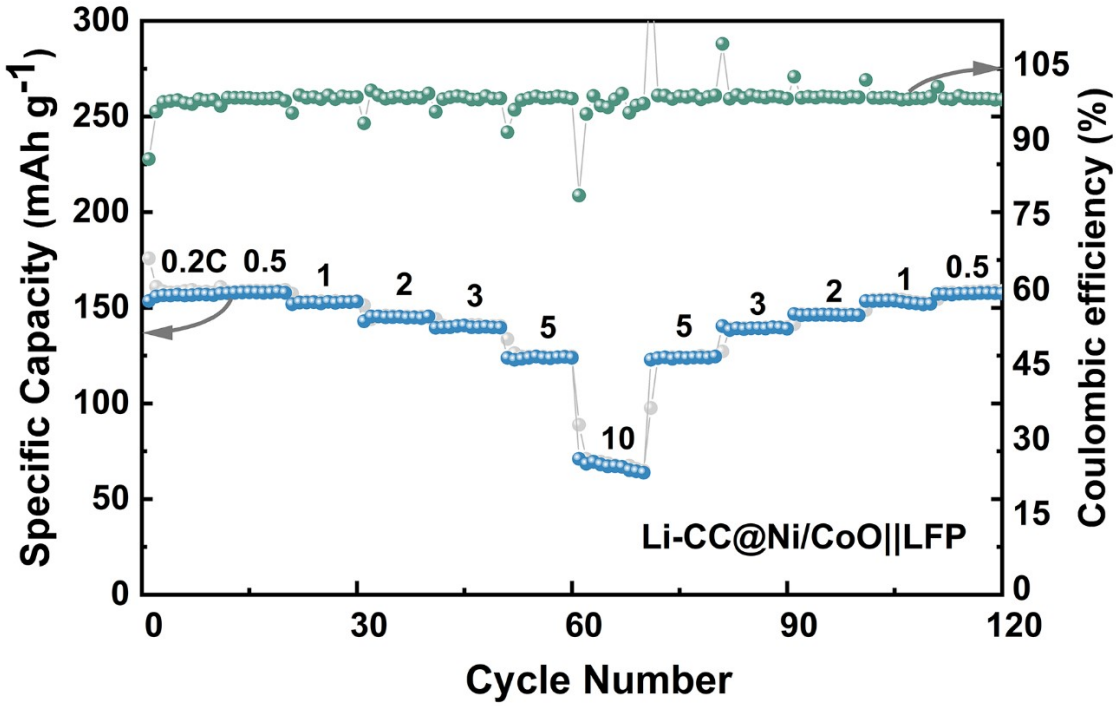

Fig. S14 Rate capability of the Li-CC@Ni/CoO||LFP full cell

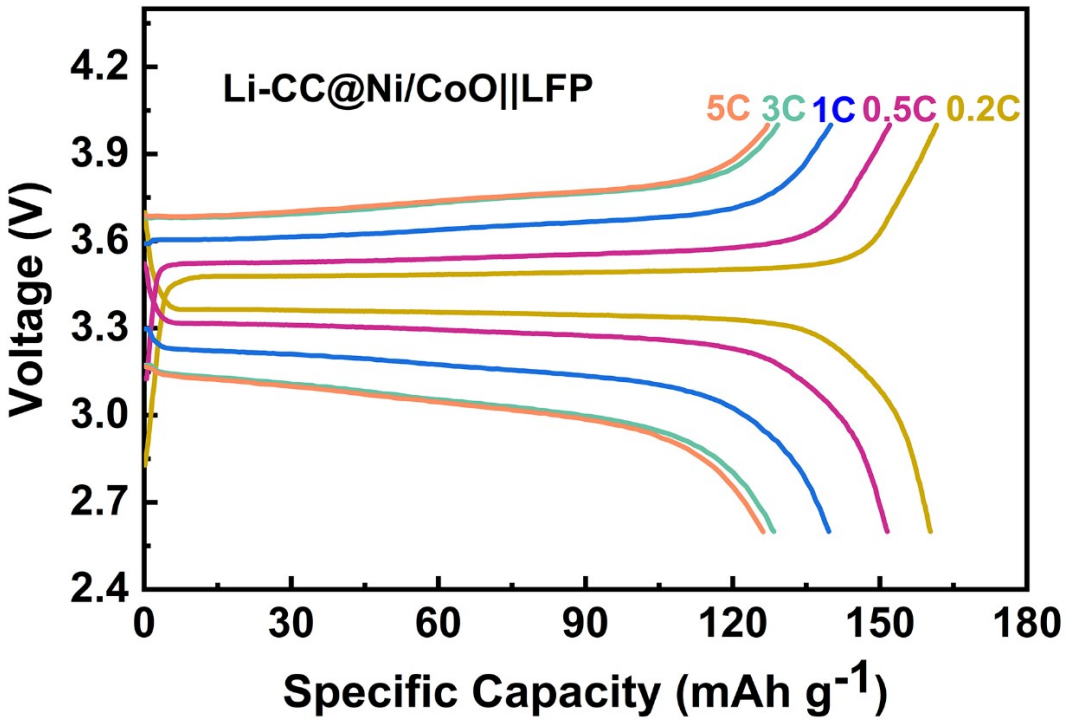

Fig. S15 Charge-discharge profiles of the Li-CC@Ni/CoO||LFP full cell from 0.2 C to 5 C

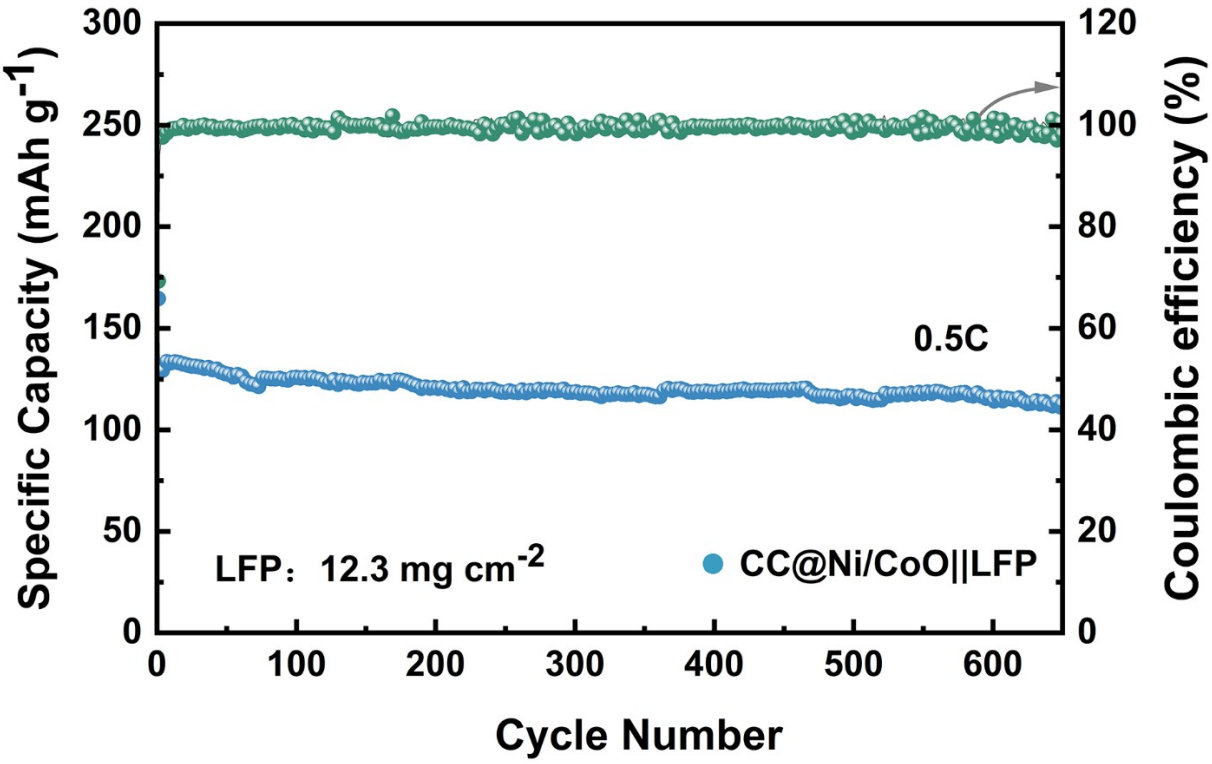

Fig. S16 CC@Ni/CoO||LFP anode free-cell performed at 0.5 C

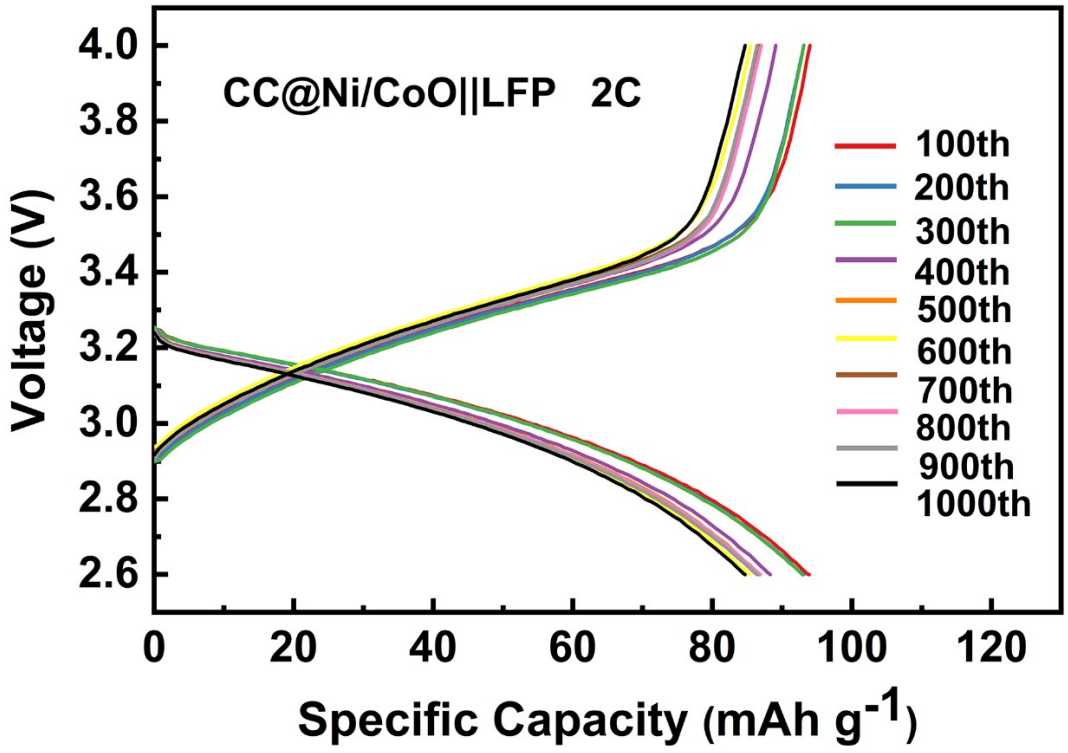

Fig. S17 Charge-discharge profiles of the CC@Ni/CoO||LFP full cell at 2 C

Table S1 Electrochemical impedance fitting results of symmetric Li cells with different electrodes

	R_1 / Ω	R_2 / Ω	R_{total} / Ω
CC(before)	1.702	169.7	171.402
CC(after)	3.208	39.28	42.488
Ni/CoO(before)	2.82	21.44	24.26
Ni/CoO(after)	2.868	7.832	10.7

Notes: R_1: electrolyte resistance; CPE: constant phase element; W_1: Warburg element(short). R_2: representing interfacial resistance between the electrode and the electrolyte, including contributions from surface film formation (R_f) and charge transfer (R_{ct}), $R_{total}=R_1+R_2$.

Table S2 Summary of the cycling performance of AFLMBs with different current collector modification strategies

Anode	Electrolyte	Rate (C)	Cycle number	Capacity retention	Ref.
CC@Ni/CoO	**1.0 M $LiPF_6$ in EC:DMC:EMC (1:1:1 wt%)**	**0.5 C** **2 C**	**650** **1000**	**93.98 %** **91.88 %**	**This work**
CTN-60	1 M LiTFSI in DOL/DME = 1:1 vol% with 2% $LiNO_3$	0.5 C	50	29 %	S1
P-Cu	1 M LiTFSI in DOL/DME with 5% $LiNO_3$	1 C	80	-	S2
Ag-PCP|Cu	0.04 M EDOT with 0.1 M $LiClO_4$ and ACN	1C	200	72 %	S3
Zn_3N_2@Cu	1 M LiTFSI in DOL/DME (v/v = 1:1) with added 1.0 wt % $LiNO_3$	0.5C	100	63.1 %	S4
Cu@PEO	1 M LiTFSI, DME/DOL (1/1, v/v) and 2 wt% $LiNO_3$	0.2C	200	30 %	S5
Au@3D-Cu	2 M LiTFSI in DOL/DME with 2 wt% $LiNO_3$	0.1C	100	45 %	S6
a-RF@3D-CM	1 M LiTFSI in DOL/DME with 2 wt% $LiNO_3$	0.2C	100	60.66 %	S7
MLG	1 M LiTFSI in DOL/DME 2% $LiNO_3$	0.2C	100	61 %	S8
HPCu	1 M LiTFSI in DOL/ DME with 2% $LiNO_3$	0.2C	100	55.5 %	S9
ICM Cu	1M LiPF6 in EC/DEC (1:1, v/v) with 10 wt% FEC	0.2C/ 0.3C	100	75.9 %	S10

Abbreviations: LiTFSI: Lithium bis(trifluoromethanesulfonyl)imide; DOL: 1, 3-dioxolane; DME: 1, 2-Dimethoxyethane; EDOT: 3,4-ethylenedioxythiophene; CAN: acetonitrile; FEC: Fuoroethylene carbonate; EC: Ethylene carbonate; DEC: Diethyl carbonate; LFP: $LiFePO_4$

References

S1 Z. Fang, S. Ding, G. Du, Y. Zhu, C. A. Serra, B. Xu, Q. Su, G. Suo and W. Wang, *J. Mater. Chem. A*, 2023, **11**, 25715–25723.

S2 Z. Sun, Y. Wang, Y. Qin, P. Yang, H. Wu, X. Li, X. Hu, C. Xiao, H. Zhao, M. Ma, Y. Su and S. Ding, *Energy Storage Mater.*, 2023, **58**, 110–122.

S3 S. Pyo, S. Ryu, Y. J. Gong, J. Cho, H. Yun, H. Kim, J. Lee, B. Min, Y. Choi, J. Yoo and Y. S. Kim, *Adv. Energy Mater.*, 2023, **13**, 2203573.

S4 Y. Zhu, S. Wu, L. Zhang, B. Zhang and B. Liao, *ACS Appl. Mater. Interfaces*, 2023, **15**, 43145–43158.

S5 A. A. Assegie, J.-H. Cheng, L.-M. Kuo, W.-N. Su and B.-J. Hwang, *Nanoscale*, 2018, **10**, 6125–6138.

S6 E. Kim, W. Choi, S. Ryu, Y. Yun, S. Jo and J. Yoo, *J. Alloys Compd.*, 2023, **966**, 171393.

S7 N. Li, T. Jia, Y. Liu, Y. Ouyang, Y. Lv, G. Zhong, Y. Wang, B. Sun, S. Lu, S. Huang, F. Kang and Y. Cao, *Mater. Today Energy*, 2023, **36**, 101341.

S8 A. A. Assegie, C.-C. Chung, M.-C. Tsai, W.-N. Su, C.-W. Chen and B.-J. Hwang, *Nanoscale*, 2019, **11**, 2710–2720.

S9 S. Zhang, J. Zeng, Y. Ma, Y. Zhao, Y. Qian, L. Suo, J. Huang, X. Wang, W. Li and B. Zhang, *Electrochimica Acta*, 2023, **442**, 141895.

S10 X. Song, C. Liu, A. Zhang, L. Ding, T. Zeng, Y. Lu, Y. Ou, W. Hou, P. Zhou, Q. Cao, S. Yan, Z. Liu, X. Peng, H. Zhou, Y. Xia, W. Zhang, H. Liu and K. Liu, *Adv. Mater.*, 2025, **37**, 2500478.